ACERP: Vol. 5, No.3, (Summer 2019) 1-7

Advanced Ceramics Progress

Research Article

Journal Homepage: www.acerp.ir

The Crystallization Effect on the Optical Properties of Oxyfluoride Glass-Ceramics Containing CaF_2 Nanocrystals Doped with Y^{3+} Ions

L. Farahinia [a], M. Rezvani [a] *

[a] *Department of Materials Science and Engineering, University of Tabriz, Tabriz, Iran*

PAPER INFO

Paper history:

Received 21 Agust 2019
Accepted in revised form 05 September 2019

Keywords:

Band Gap Energy
Urbach Tailing
Y_2O_3 Dopant
Oxyfluoride Glass

ABSTRACT

In the present study, the oxyfluoride glasses of SiO_2-Al_2O_3-CaF_2 system containing different amounts of Y^{3+} ions were prepared through the convenient melting method. The crystallization temperatures and size of the CaF_2 nanocrystals were obtained from DTA curves and XRD patterns, respectively. As a consequence, the optimum amount of Y_2O_3 dopant (0.5wt%) and the suitable composition for basic glass were determined from the viewpoints of better crystallization behavior and higher transparency. The FTIR spectra approved the presence of oxyfluoride glass-ceramic structure in samples. The optical parameters (Fermi energy level, Urbach energy, direct and indirect band gaps) were calculated using UV-Vis spectra. The decreasing trend of Fermi energy level for glass-ceramic samples crystallized at higher temperatures is related to better semiconducting behavior. Urbach energy and optical band gap of the glass-ceramic samples were reduced due to the increment of the structural order and the emergence of dangling bonds, respectively.

1. INTRODUCTION

Recently, transparent oxyfluoride glass-ceramics have been extensively investigated due to their potential applications in photonic devices such as optical fiber amplifiers, lasers, planar optical waveguide, and so on [1-5]. Oxyfluoride glass-ceramics are attractive materials due to their higher mechanical, chemical, and thermal stability than fluoride glasses and lower phonon energy than oxide glasses [6-7]. Wang and Ohwaki (1993) [8] presented the first oxyfluoride glass-ceramic containing $Pb_xCd_{1-x}F_2$ crystalline phase doped with Er^{3+} and Yb^{3+} ions. They found out that the red emission from Er^{3+} ions is dominant for the glass-ceramics, but not for glasses. They ascribed this difference to the higher energy transfer or cross-relaxation rate between Er^{3+} and Yb^{3+} ions in the glass-ceramic samples [8]. After this pioneering work, different nanocrystals of fluorides such as LaF_3, PbF_2, CdF_2, and MF_2 (M= Ca, Ba, and Sr) are precipitated in the oxyfluoride glass-ceramics [9-10]. However, their applications are limited due to the harmful effects of CdF_2 and PbF_2 on the environment [11]. Dejneka [12] introduced a new kind of oxyfluoride glass-ceramics based on LaF_3 crystals. In contrary to the fact that the efficiency of induced luminescence of this kind of glass-ceramics is comparable to Schott IQI-301 products, the high-cost LaF_3 is an obstacle for their practical applications [11]. Fu et al [13] reported the oxyfluoride glass-ceramics containing CaF_2 nanocrystals for the first time, which received great attention these days. Among the different fluoride nanocrystals precipitated in these glass-ceramics, CaF_2 is more preferable due to the high transparency to wavelengths from 0.13 to 9.5μm. Moreover, CaF_2 nanocrystals have high refractive index compatibility with the aluminosilicate glass matrix. Besides, the lower cost and toxicity of CaF_2 resulted in more interest of researchers in oxyfluoride glass-ceramics containing CaF_2 crystals for improving their optical applications [14-15].

A considerable number of studies have been carried out on the effects of rare-earth ions on the optical properties of oxyfluoride glass and glass-ceramics, like luminescence properties, upconversion behavior and other optical properties. Among the different rare-earth ions, Y^{3+} ions are important because of their surrounding ligand field of 4f-electrons, which

*Corresponding Author Email: m_rezvani@tabrizu.ac.ir (M. Rezvani)

influence the optical properties, like semiconducting behavior [16]. Although the effects of Y^{3+} ions on the optical semiconducting behavior of other glass-ceramic systems [17-18] have been studied, there is not any report of using these ions in oxyfluoride glass-ceramics. Thus, the optical semiconducting properties of oxyfluoride glass-ceramics were studied in the present work after choosing a suitable amount of Y_2O_3 dopant.

2. EXPERIMENTAL PROCEDURE

The composition of the basic glasses (weight ratio) is presented in Table 1. CaO is also added to the three main constituents, i.e., SiO_2, Al_2O_3, and CaF_2.
Replacing some amounts of CaF_2 by CaO prevents the loss of F^- ions [11].

TABLE 1. Compositions of glasses containing different amounts of Y_2O_3 (weight ratio)

Composition / Sample Code	SiO_2	Al_2O_3	CaO	CaF_2	Y_2O_3	As_2O_3	Sb_2O_3
GY0.5	37.26	28.11	7.73	26.89	0.5	0.2	0.2
GY1	37.26	28.11	7.73	26.89	1	0.2	0.2
GY1.5	37.26	28.11	7.73	26.89	1.5	0.2	0.2

Leached SiO_2 with high purity, Al_2O_3 (Merck 101077), CaF_2 (Dae Jung 2508145) and $CaCO_3$ (Merck 102069) were used as the starting materials of main components. As_2O_3 (Merck 1001190100) and Sb_2O_3 (Acros 213471000) were also supplied as refining agents to produce bubble-free samples. Different amounts of Y_2O_3 (Merck 112412), i.e., 0.5, 1, and 1.5 (weight ratio), were added to introduce the Y^{3+} ions.
50g of three batches were mixed and melted in alumina crucibles at 1450°C for 1 hour in an electric furnace. Crucibles were covered by alumina plates and quite high heating rate for the melting process (15°C/min) was applied to control the fluoride loss. Then, the preheated stainless steel molds were used to shape the molten glasses at 500°C. Finally, the glassy discs with 0.5cm thickness were prepared. Annealing at 500°C for 30 min was carried out for releasing the internal stresses of samples. The crystallization temperatures were determined according to the differential thermal analysis (DTG-60AH Shimadzu) results (heating rate of $10°C.min^{-1}$). Glass-ceramic samples were prepared through the crystallization of glasses at different temperatures starting from crystallization peak temperature to 850°C. The precipitated crystalline phase in glass-ceramics was identified by X-ray diffraction (XRD, Siemens D-500) patterns.
The optical transmittance measurements were carried out in the UV-Vis spectrum range using a UV-Vis Shimadzu 1700 spectrophotometer instrument at ambient temperature. The absorption and extinction coefficient, Fermi energy level, direct and indirect optical band gaps, and Urbach energy of the samples were determined according to the results obtained from transmittance spectra.

3. RESULTS AND DISCUSSION

3.1. Determination of optimum amount of Y_2O_3 dopant

The XRD patterns of the basic glasses and the attributed glass-ceramic samples are shown in Fig. 1. The glassy samples do not show any peak due to the amorphous structure. In other word, no unwanted crystallization occurred during the processing procedure. According to previous results [19], (DTA curves of glasses containing different amounts of Y_2O_3) two distinguishable exothermic peaks are observed, which are attributed to the crystallization of CaF_2 and anorthite, respectively.
Therefore, the glasses containing different amounts of Y_2O_3 were heat-treated at the first peak temperature (T_{P1}) of samples for 2 hours. The XRD patterns approved the precipitation of CaF_2 in these samples (GCY0.5-690, GCY1-700, and GCY1.5-719). Hence, glasses were heat-treated at different temperatures ranging from T_{P1} to 850˚C with the steps of 25˚C to prepare suitable glass-ceramic samples. Since temperatures higher than 850˚C did not result in transparent samples, no glass-ceramic was prepared at higher temperatures. The crystallization conditions and code of samples are tabulated in Table 2.
As shown in Fig. 2, all of the peaks in XRD results of crystallized samples are assigned to CaF_2 nanocrystals (ICDD: 00-35-0816). Moreover, Scherer's equation (Eq. 1) was used to calculate the crystal size of CaF_2 crystals embedded in the glassy matrix.

$$D = \frac{0.9\lambda}{B\cos\theta_B} \quad (1)$$

Where D is crystal size, λ is the wavelength of X-ray (Cu Kα: 1.541 Å), θ_B is the diffraction angle, and B is the width of the diffraction peak at the half maximum. The peaks get sharper with increasing the crystallization temperature, which indicates the gradual formation of CaF_2 nanocrystals in the glass-ceramics.
Higher Y_2O_3 has resulted in larger crystals in glass-ceramics prepared at the same temperature (Table 2). This outcome is related to the mechanism suggested by Russel [20] for the crystallization of CaF_2. Russel pointed to an interface, which is formed near the crystals and enriched of glass formers. This interface hinders the diffusion and prevents the more crystallization of CaF_2. Since Y_2O_3 leads to a higher

viscosity, diffusion gets difficult through the interface and consequently, CaF_2 crystals get smaller. As a result, the higher amount of Y_2O_3 increases the crystallization temperature and smaller CaF_2 crystals.Considering both crystallization temperature and CaF_2 crystals size due to the moderate properties of GY0.5 glass, it has been chosen as the favorable composition. On the other hand, glass-ceramic samples prepared from GY0.5 glass were chosen for further optical studies with a mean crystal size under 30nm and suitable transparency.

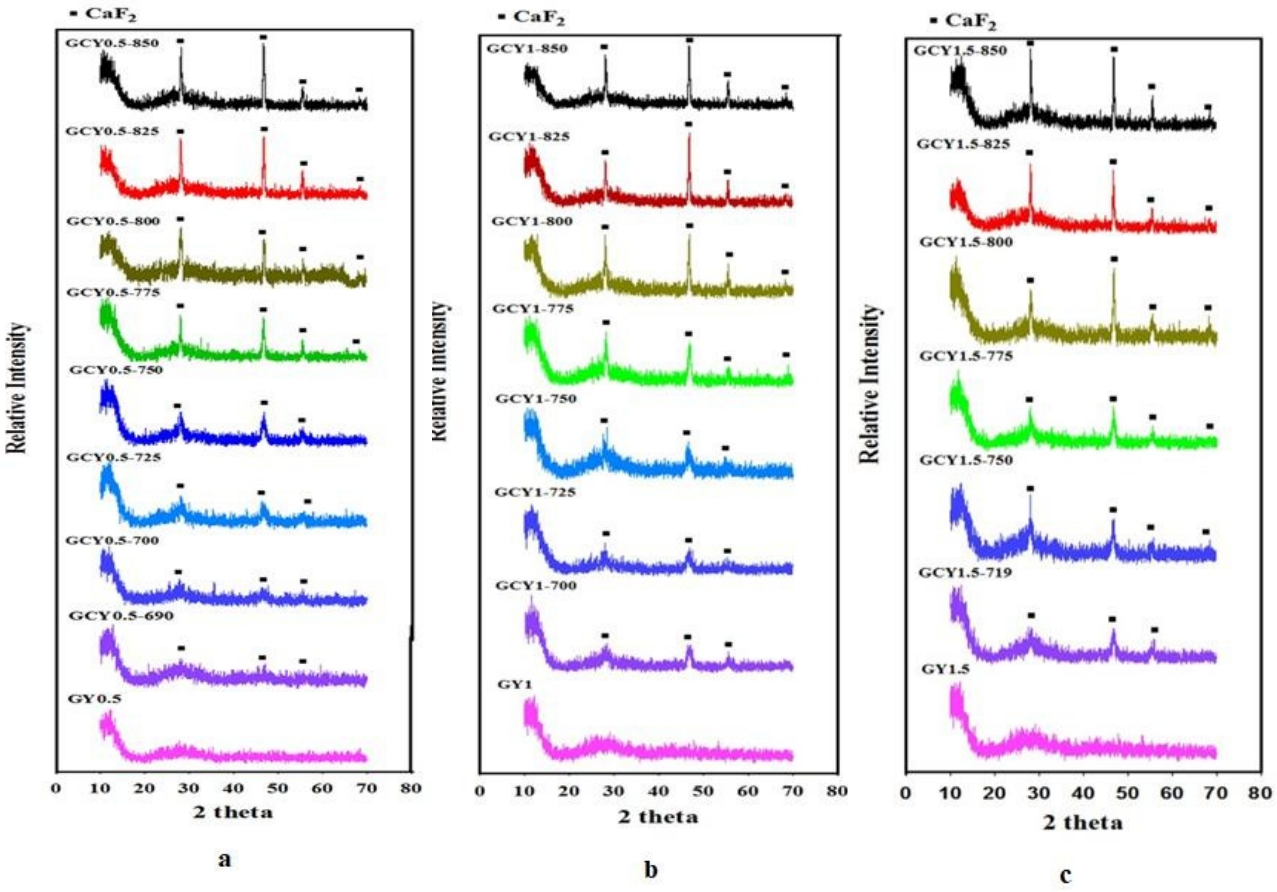

Figure 1. XRD patterns of glasses and glass-ceramics containing (a) 0.5, (b) 1, and (c) 1.5 weight ratio of Y_2O_3

3.2. FTIR spectroscopy

FTIR spectroscopy was carried out to study the structure of samples. Fig. 2 presents the FTIR spectra of GY0.5 and the glass-ceramics. Since SiO_2 is one of the main components of the basic glass composition, bands related to the presence of SiO_4 tetrahedra in the glass network. Therefore, peaks placed at the ~460, ~700, and ~1170cm^{-1} are attributed to the rocking vibrations, symmetric stretching vibrations, and asymmetric stretching vibrations of Si-O-Si bonds [21-22]. Si^{4+} ions are replaced by Al^{3+} ions, which act as network formers and results in Al-O-Si bonds. Therefore, the absorptions at ~1060 and ~560cm^{-1} are related to the asymmetric stretching vibration mode of Si-O-Al [23]. Ca-F bonds should have resulted in a peak at 443.30cm^{-1} [24], which is overlapped with the rocking vibration mode of Si-O-Si. Thus, it is somehow difficult to distinguish this peak.

Furthermore, the peaks relating to Ca-F bond gets intensified by the increase of crystallization temperature, which is caused by more crystallization of CaF_2 crystals in glass-ceramics. In oxyfluoride glasses, F^- ions associated with aluminum atoms in AlO_4 tetrahedra [25]. Therefore, Al-F bonds create a peak at about 1350 and 1750 cm^{-1} in FTIR spectra [26]. On the other hand, Ca^{2+} ions attempt to compensate the negative charge induced in both $[AlO_4]^-$ and $[AlO_3F]^-$ tetrahedral and create a band at ~990cm^{-1} related to Si-O-Ca bonds due to the replacing oxygen by F^- [21]. The peak observed at 3500cm^{-1} may be emerged due to the O–H stretching of the surface water. According to Fig. 2, the higher

crystallization temperature has resulted in more intensified peaks. Since FTIR is a vibrational technique, the overall spectrum of crystalline material will have much sharper bands than the spectrum of amorphous material.

TABLE 2. Crystallization condition and crystal size of glass-ceramic samples

Sample Code	Crystallization Temperature (°C)	Crystal Size (nm)
GCY0.5-690	690	10.53
GCY0.5-700	700	15.60
GCY0.5-725	725	17.07
GCY0.5-750	750	20.39
GCY0.5-775	775	33.56
GCY0.5-800	800	41.75
GCY0.5-825	825	49.09
GCY0.5-850	850	49.74
GCY1-700	700	14.65
GCY1-725	725	15.99
GCY1-750	750	18.29
GCY1-775	775	28.71
GCY1-800	800	35.21
GCY1-825	825	47.00
GCY1-850	850	48.77
GCY1.5-719	719	12.58
GCY1.5-750	750	14.73
GCY1.5-775	775	18.83
GCY1.5-800	800	32.49
GCY1.5-825	825	47.23
GCY1.5-850	850	48.18

3.3. Evaluation of optical constants

3.3.1. Determination of fermi energy level

UV-Vis absorption spectra of oxyfluoride glass and glass-ceramics are presented in Fig. 3. In contrary to the basic glass, the absorption edge becomes more intensive for glass-ceramics, which means absorption edge increases with crystallization [27] and shifts to longer wavelength. It may be caused by the reduced number of non-bridging fluorine (NBF) in the residual glassy phase when the CaF_2 crystalline phase precipitates [28].

According to the Strong absorption of UV absorption bonds, extinction coefficient (*K*) obeys from the Fermi-Dirac distribution function, thus, the Fermi energy level can be calculated by applying the following equation (2):

$$K(\lambda) = \frac{1}{1+\exp\left(\frac{E_f - E}{K_B T}\right)} \quad (2)$$

Where is E_f the Fermi energy, E is the variable photon energy, k_B is the Boltzmann constant and T is the ambient temperature (297K) [29-31]. Fig. 4 depicts K vs. hυ plots for different glass samples. The calculated values for the Fermi energy of samples are presented in Table 3, which are achieved from least-square fittings of (Eq. 2). The reduction of Fermi energy level with higher crystallization temperatures indicates a change to better semiconducting properties in glass-ceramic samples.

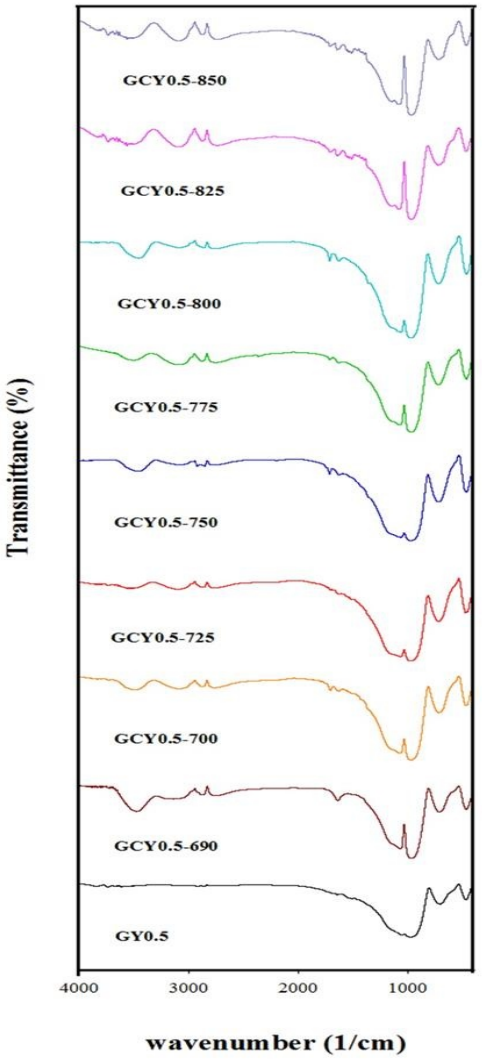

Figure 2. FTIR spectra of glass GY0.5 and corresponding glass-ceramics

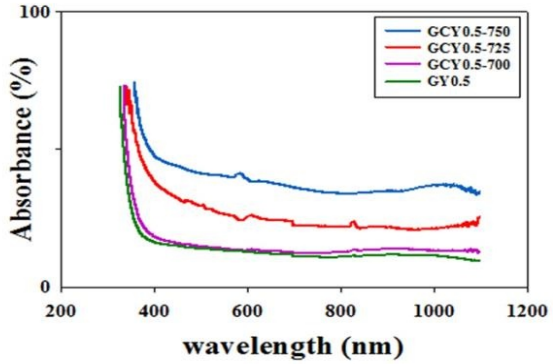

Figure 3. UV- Vis spectra of glass GY0.5 and corresponding glass-ceramics

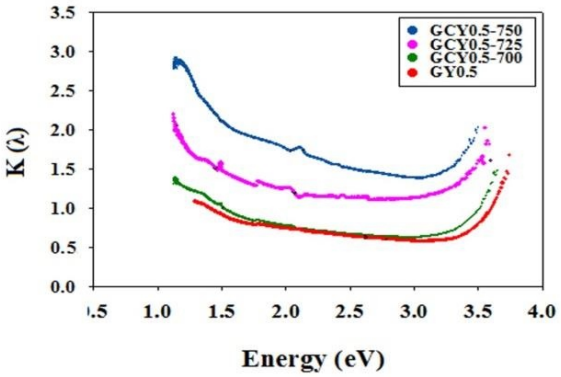

Figure 4. Extinction coefficient vs. energy plots of glasses heat-treated at different temperatures

TABLE 3. Optical properties of oxyfluoride glasses heat-treated at different temperatures

Sample \ Energy (eV)	E_f	$E_{indirect}$	E_{direct}	E_U
GY0.5	3.59	3.57	3.00	0.27
GCY0.5-700	3.57	3.25	2.61	0.23
GCY0.5-725	3.53	3.32	2.28	0.22
GCY0.5-750	3.40	2.90	2.13	0.18

3.3.2. The direct and indirect optical band gap

The absorption coefficient exhibits a sharp increase for amorphous materials just before the band gap. The relation between the absorption coefficient and the incident photon energy is given by the following equation:

$$\alpha = \beta^2 \frac{(h\upsilon - E_g^{opt})^n}{h\upsilon} \quad (3)$$

Where, β is a constant related to the extent of the band tailing, n is the index, which can have different values as much as 2, 3, 1/2, and 1/3 corresponding to indirect allowed, indirect forbidden, direct allowed, and direct forbidden transitions, respectively [32]. Therefore, the intercept of the obtained line divided by slope, is equal to the energy band gap of optical transitions through the plot $(\alpha h\upsilon)^{1/n}$ vs. Photon energy (Tauc's plots). Fig. 5 illustrates the Tauc's plots of samples and Table 3 shows the direct and indirect allowed optical band gaps of the samples calculated from these plots. Optical band gap decreases in glass-ceramics crystallized at higher temperatures. The crystallization and formation of crystals in the glassy matrix cause the creation of energy levels in the forbidden gap that could reduce the band gap of samples. This reduction is due to the decrease in average bond energy and fall in conduction band's level [29]. On the other hand, the reduction in band gap energy could be interpreted by assuming the production of surface dangling bonds around crystallites during the process of crystallization [33]. It has been suggested that dangling bonds are produced around the surface of crystallites when crystallization occurs in amorphous materials. Thereby, the number of surface dangling bonds increase by increasing the crystallization temperature. Increment of dangling bonds leads to the formation of more localized states in the band structure and consequently, the reduction of the optical energy gap [34].

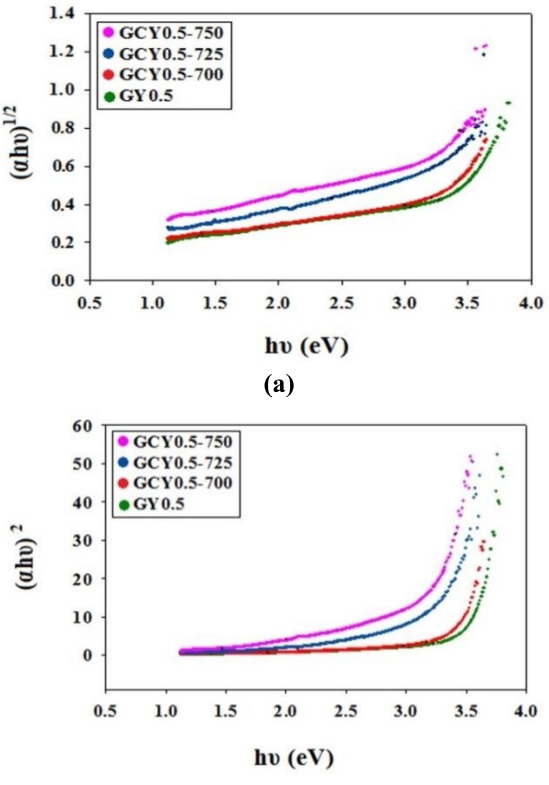

Figure 5. Tauc' plots for (a) indirect and (b) direct band gap of glasses heat-treated at different temperatures

3.3.3. Urbach energy

The optical absorption in amorphous semiconductors near the absorption edge is usually characterized by three types of optical transitions corresponding to transitions between tail and tail states, tail and extended states, and extended and extended states. The first two types correspond to $h\nu \leq E_g^{opt}$ and the third one corresponds to $h\nu \geq E_g^{opt}$. Thus, the plot of the absorption coefficient versus photon energy (α vs. hν) has three different regions. In the second region, the absorptions are related to transitions from the localized tail states above the valence band edge to extended states in the conduction band and/or from extended states in the valence band to localized tail states below the conduction band. The spectral dependence of the absorption coefficient usually follows the so-called Urbach rule (Eq. 4).

$$\alpha = \beta \exp(\frac{h\upsilon}{E_U}) \quad (4)$$

Therefore, Urbach energy (E_U) has been calculated using Eq. 4 and least square fitting of Ln(α) against hν curves in the tailing part of localized states (Fig. 6) [35-38]. Table 3 represents the Urbach energy values of the samples, which decreases in the case of crystallization at higher temperatures. Since the Urbach energy of glassy semiconductors implicitly defines the degree of disorder, the crystallization and resulted order of this process decrease the Urbach energy in value.

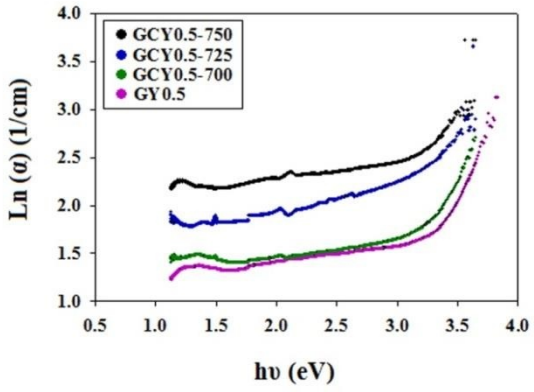

Figure 6. Determination of Urbach energy of glasses heat-treated at different temperatures

4. CONCLUSIONS

1. Oxyfluoride glasses doped with different amounts of Y_2O_3 were prepared using convenient melting process. Considering DTA patterns, crystallization temperatures of samples were determined and glass-ceramic samples containing CaF_2:Y^{3+} nanocrystals were obtained.
2. The suitable composition for the basic glass was chosen according to the effect of Y_2O_3 dopant on the crystallization temperature and crystal size of CaF_2.
3. Higher crystallization temperatures resulted in glass-ceramic samples with more semiconducting properties. To put it another way, the Fermi energy level was decreased from 4.29 to 3.07eV.
4. Creation of energy level in the band gap and the presence of dangling bonds are 2 possible reasons for the reduction of band gap energies.
5. Higher crystallization temperature decreased Urbach band tailing from 0.27 to 0.18eV due to the higher crystallinity.

5. ACKNOWLEDGEMENTS

We would like to show our gratitude to Farhad Ghanbari, the chemistry service laboratory assistant of University of Tabriz for assistance with spectroscopic analyses of this paper.

REFERENCES

1. Fedorov, P.P., Luginina, A. A., Popov, A. I., "Transparent oxyfluoride glass ceramics", ***Journal of Fluorine Chemisty***, Vol. 172, (2015), 22-50.
2. Polosan, S., Secu, C. E., "Optical properties of CaF_2:Eu^{3+} nanocrystals embedded in transparent oxyfluoride glass ceramic", ***Journal of Optoelectronics and Advanced Materials***, Vol. 10, No. 8, (2008), 2134-2137.
3. Beall, G. H., Duke, D. A., "Transparent glass-ceramics", ***Journal of Materials Science***, Vol. 4, (1969), 340-352.
4. Shinozaki, K., Honma, T., Oh-ishi, K., Komatsu, T., "Fluorine deficient layer at the surface of transparent glass-ceramics with CaF_2 nanocrystals", ***Journal of Physics and Chemistry of Solids***, Vol. 73, (2012), 683-687.
5. Babu, P., Jang, K. H., Rao, C.S., Shi, L., Jayasankar, C.K., Lavín, V., Seo, H.J., "White light generation in Dy^{3+}-doped oxyfluoride glass and transparent glass-ceramics containing CaF_2 nanocrystals", ***Optics express***, Vol. 19, (2011), 1836-1841.
6. Qiao, X., Fan, X., Wang, J., Wang, M., "Luminescence behavior of Er^{3+} ions in glass–ceramics containing CaF_2 nanocrystals", ***Journal of Non-Crystalline Solids***, Vol. 351, (2005), 357-363.
7. Kishi, Y., Tanabe, S., "Infrared-to-visible upconversion of rare-earth doped glass ceramics containing CaF_2 crystals", ***Journal of alloys and compounds***, Vol. 408, (2006), 842-844.
8. Wang, Y., Ohwaki, J., "New transparent vitroceramics codoped with Er^{3+} and Yb^{3+} for efficient frequency upconversion", ***Applied Physics Letters***, Vol. 63, No. 24, (1993), 3268-3270.
9. Fedotovs, A., Antuzevics, A., Rogulis, U., Kemere, M., Ignatans, R., "Electron paramagnetic resonance and magnetic circular dichroism of Gd^{3+} ions in oxyfluoride glass-ceramics containing CaF_2 nanocrystals", ***Journal of Non-Crystalline Solids***, Vol. 429, (2015), 118-121.
10. Liu, M., Zhao, L., Liu, Y., Lan, Z., Chang, L., Li, Y., Yu, H., "Role of heavy metal ions in the formation of oxyfluoride

glasses and glass ceramics", ***Journal of Materials Science & Technology***, Vol. 30, No. 12, (2014), 1213-1216.

11. Imanieh, M. H., Eftekhari Yekta, B., Marghussian, V., Shakhesi, S., Martin, I. R., "Crystallization of nano calcium fluoride in CaF_2-Al_2O_3-SiO_2 system", ***Solid State Sciences***, Vol. 17, (2013), 76-82.
12. Dejneka, M. J., "The luminescence and structure of novel transparent oxyfluoride glass-ceramics", ***Journal of Non-Crystalline Solids***, Vol. 239, (1998), 149-155.
13. Fu, J., Parker, J. M., Flower, P. S., Brown, R. M., "Eu^{3+} ions and CaF_2-containing transparent glass-ceramics", ***Materials Research Bulletin***, Vol. 37, (2002), 1843-1849.
14. Chen, D., Wang, Y., Ma, E., Yu, Y., Liu, F., "Partition, luminescence and energy transfer of Er^{3+}/Yb^{3+} ions in oxyfluoride glass ceramic containing CaF_2 nano-crystals", ***Optical Materials***, Vol. 29, (2007), 1693-1699.
15. Hu, Z., Wang, Y., Ma, E., Chen, D., Bao, F., "Microstructures and upconversion luminescence of Er^{3+} doped and Er^{3+}/Yb^{3+} co-doped oxyfluoride glass ceramics", ***Materials chemistry and physics***, Vol. 101, (2007), 234-237.
16. Shakeri, M. S., Rezvani, M., "Optical band gap and spectroscopic study of lithium alumino silicate glass containing Y^{3+} ions", ***Spectrochimica Acta Part A: Molecular and Biomolecular Spectroscopy***, Vol. 79, (2011), 1920-1925.
17. Singh, S., Kalia, G., Singh, K., "Effect of intermediate oxide (Y_2O_3) on thermal, structural and optical properties of lithium borosilicate glasses", ***Journal of Molecular Structure***, Vol. 1086, (2015), 239-245.
18. Kaur, G., Kumar, M., Arora, A., Pandey, O. P., Singh, K., "Influence of Y_2O_3 on structural and optical properties of SiO_2-BaO-ZnO-xB_2O_3-(10-x) Y_2O_3 glasses and glass ceramics", ***Journal of Non-Crystalline Solids***, Vol. 357, (2011), 858-863.
19. Farahinia, L., Rezvani, M., "Optical property evaluation of oxyfluoride glasses doped with different amounts of Y^{3+} ions", ***Journal of Non-Crystalline Solids***, Vol. 425, (2015), 158-162.
20. Russel, C., "Nanocrystallization of CaF_2 from $Na_2O/K_2O/CaO/CaF_2/Al_2O_3/SiO_2$ glasses", ***Chemistry of Materials.***, Vol. 17, (2005), 5843-5847.
21. Mukherjee, D. P., Kumar Das, S., "Effects of nano silica on synthesis and properties of glass ceramics in SiO_2-Al_2O_3-CaO-CaF_2 glass system: A comparison,", ***Journal of Non-Crystalline Solids***, Vol. 368, (2013), 98-104.
22. Atalay, S., Adiguzel, H. I., Atalay, F., "Infrared absorption study of Fe_2O_3–CaO–SiO_2 glass ceramics", ***Materials Science and Engineering: A***, Vol. 304, (2001), 796-799.
23. Groß, U., Rüdiger, S., Kemnitz, E., "Alkaline earth fluorides and their complexes: A sol-gel fluorination study", ***Solid State Sciences***, Vol. 9, (2007), 838-842.
24. Tahvildari, K., Ghammamy, Sh., Nabipour, H., "CaF_2 nanoparticles: Synthesis and characterization", ***International Journal of Nano Dimension***, Vol. 2, (2012), 269-273
25. Hill, R., Wood, D. , Thomas, M., "Trimethylsilylation analysis of the silicate structure of fluoro-aluminosilicate glasses and the structural role of fluorine", ***Journal of materials science***, Vol. 34, (1999), 1767-1774.
26. Zhang, Y., Chen, D., "Multilayer integrated film bulk acoustic resonators", Springer, Shanghai, (2013).
27. Faeghi Nia, A., "UV-Vis Absorption and Luminescence Spectrum of LAS: Tb^{3+}/Gd^{3+} as a Laser Material", ***International Journal of Engineering***, Vol. 4, (2014), 609-614.
28. Sun, X., Gu, M., Huang, Sh., Jin, X., Liu, X., Liu, B., Ni, Ch., "Luminescence behavior of Tb^{3+} ions in transparent glass and glass- ceramics containing CaF_2 nanocrystals", ***Journal of Luminescence***, Vol. 129, (2009), 773-777.
29. El-Diasty, F., Abdel Wahab, F. A., Abdel- Baki, M., "Optical band gap studies on lithium aluminum silicate glasses doped with Cr^{3+} ions", ***Journal of applied physics***, Vol. 100, (2006), 093511.
30. Khashan, M. A., El-Naggar, A. M., "A new method of finding the optical constants of a solid from the reflectance and transmittance spectrograms of its slab", ***Optics Communications***, Vol. 174, (2000), 445–453.
31. El-Kameesy, S. U., Eissa, H. M., Eman, S. A., El-Gamma, Y. A., "Fast Neutron Irradiation Effect on Some Optical Properties of Lead Borate Glass Doped with Samarium Oxide", ***Egyptian Journal of Basic and Applied Sciences***, Vol. 49, (2011), 67-70.
32. Mott, N. F., Davis, E. A., "Electronic processes in nanocrystalline materials", Oxford university press, (2012).
33. Dwivedi, D. K., Pathak, H. P., Shukla, N., Kumar, A., "Effect of thermal annealing on structure and the optical band gap of amorphous Se 75-x Te 25 Sb x thin films by vacuum evaporation technique.", ***Journal of Ovonic Research***, Vol. 10, (2014), 15-22.
34. Hasegawa, S., Kitagawa, M., "Effects of annealing on localized states in amorphous Ge films", ***Solid State Communications***, Vol. 27, (1978), 855-858.
35. Rani, S., Sanghi, S., Agarwal, A., Seth, V. P., "Study of optical band gap and FTIR spectroscopy of $Li_2O.Bi_2O_3.P_2O_5$ glasses", ***Spectrochimica Acta Part A: Molecular and Biomolecular Spectroscopy***, Vol. 74, (2009), 673-677.
36. Babanejad, S. A., Ashrafi, F., Salarzadeh, N., Ashrafi, E., "Study the Optical properties of Amorphous Structure (Glassy) of B_2O_3-CdO Binary System", ***Advances in Applied Science Research***, Vol. 3, (2012), 743-748.
37. Al-Ghamdi,A. A., Khan, Sh. A., "Laser-induced changes on optical band gap of amorphous and crystallized thin films of $Se_{75}S_{25-x}AG_x$", ***Physica B: Condensed Matter***, Vol. 404, (2009), 4262-4266.
38. Subrahmanyam, K., Salagram, M., "Optical band gap studies on (55-x)Na2O-xPbO-45P2O5 (SLP) glass system", ***Optical Materials***, Vol. 15, (2000), 181-186 .